Contents lists available at ScienceDirect

Forensic Science International: Synergy

Multiple tier detection of TNT using curcumin functionalized silver nanoparticles

Ali Raza[*], Amitabh Biswas, Ali Zehra, Abdurrohman Mengesha

Department of Forensic Chemistry & Toxicology, Abaya Campus, Arba Minch University, Arba Minch, Ethiopia

ARTICLE INFO

ABSTRACT

The rapid, selective and sensitive detection of trinitrotoluene (TNT), which is widely used in terrorist activities and also a major environmental contaminant is prime concern for the scientific community dealing with environmental problems and national security. This paper described unprecedented CAgP based multiple tier probe employing U.V.–Vis., DLS & SERS techniques for highly selective, rapid and ultrasensitive detection of TNT up to 0.1 nM level. The as synthesized CAgP made possible the naked eye detection of TNT in the form of flakes in real time. The developed method due to its multiple tier approach utilizing the same sample could easily be extended to a high-throughput format and can be utilized for rapid and reliable trace detection of TNT, for on-site screenings in airports, analysis of forensic samples, and environmental analysis.

© 2020 The Authors. Published by Elsevier B.V. This is an open access article under the CC BY-NC-ND license (http://creativecommons.org/licenses/by-nc-nd/4.0/).

1. Introduction

The recent spurt in terrorist activities involving TNT as an explosive and its widely reported role as an environmental contaminant made it an analyte of prime concern for the scientific community dealing with environmental problems and national security [1–3].As a result, there is an urgent need for rapid and reliable methods of trace detection of TNT, for screenings in airports, analysis of forensic samples, and environmental analysis [4,5]. A successful chemical sensor for TNT must be extremely sensitive, highly selective, robust, miniaturized and most importantly, be able to perform real time on-site analysis. Traditionally, x-ray based instruments and trained animals are the basic choices to handle the explosives substances like TNT. Canines are still considered the gold standard for field methods of detecting explosives [2,3]. Other techniques like HPTLC, HPLC, IR & Raman spectroscopy and state-of-the art instrumentation methods like GC, electrophoresis & mass-spectrometric methods have been widely reported for the detection of explosives [3–6]. Recently, sensors based detection owing to their high sensitivity, selectivity and rapidness witnessed an explosives growth in the different sensor concepts for analyzing explosives at trace level comprising fluorescence quenching sensors, electrochemical sensors, organic dye based fluorescence resonance energy transfer (FRET), and nanotechnology based sensors. In nanotechnology derived sensors, the induced aggregation of nanoparticles (NPs) based TNT sensing has been perceived by various techniques like colorimetry, electrochemical methods, SERS DLS and miscellaneous methods [7–11]. Among all the reported TNT sensitive probes, the dynamic light scattering (DLS) and surface enhanced Raman scattering (SERS) are suitable for application purposes owing to their high sensitivity, selectivity, least expensive, minimal sample preparation and colorimetric nature [12–30]. The introduction of portable Raman spectrometer made SERS as one of the technique ready to use at the important places like airport etc for screening of explosives. Recent SERS and DLS approaches for selective and sensitive detection of TNT involve incorporation of various electron rich moieties on SERS substrate surface e.g. amine functionalized Au NPs [22,24]. Nitro derivatives are known to act as an electron acceptor and form Meisenheimer complexes when combined with electron donors such as amines. The interactions of donor amine groups (present in amine-functionalized AuNPs) with the acceptor nitro-compounds (that are employed as analytes) promote the aggregation of NPs. This aggregation of NPs resulted in enhanced SERS properties as the 'hot-spots' formation increased with more and more aggregation. The aggregation of NPs can be studied effectively by DLS method also, as the technique relied on the size of NPs. By incorporating a

* Corresponding author. Department of Forensic Chemistry & Toxicology, Abaya Campus, Arba Minch University, P.O. Box 21, Ethiopia.
E-mail address: ali.raza@amu.edu.et (A. Raza).

specific chemical moiety on the SERS surface, one can target the detection of a single species present in a complex sample mixture at nano to femto molar level without having to physically separate out interfering species. Very high selectivity and sensitivity offered by SERS, along with the highly informative spectra characteristics of Raman spectroscopy, allows SERS-based method a feasible alternative to more commonly used optical sensing methods. Pandya et al. fabricated ultrasensitive nanocurcumin based fluorescent probe for detection of trace amount of TNT with excellent sensitivity (1 nM) and selectivity over other nitro explosives *via* aggregation and reported a fluorescent enhancement, upto 800 fold [15]. They utilized the electron donating ability of the curcumin to form the curcumin-TNT Meisenheimer complex.

In this paper, we demonstrate curcumin functionalized silver nanoparticles (CAgP) based miniaturized, inexpensive ultrasensitive UV−Vis, SERS and DLS multi tier probe, for highly sensitive and selective screening of TNT. In this work, we evaluated the interaction between TNT and curcumin functionalized Ag NPs by electronic absorption, DLS and SERS study. Our approach relied on the π-donor acceptor interactions between TNT and curcumin capped on Ag NPs. Due to interaction of curcumin with TNT, the curcumin capped Ag NPs undergoes aggregation and the size of aggregates increases as the concentration of TNT increases. With increase in aggregation of Ag NPs an enhanced SERS activity and DLS detection was observed. The naked eye visible formation of silver flakes at higher concentration (0.01M) of TNT was also observed. The availability of different instruments with different organizations made our multiple tier approach for detecting TNT a practically viable method.

2. Experimental

2.1. Reagents and materials

Silver nitrate and polyvinylpyrrolidinone (PVP) were purchased from Sigma Aldrich. Ethylene glycol, curcumin, p-nitro-benzaldehyde, phenol, and toluene were purchased from SRL chemicals. Purified TNT and 2,4 DNT was a kind gift from NICFS, New Delhi, India. Stock solution of TNT, DNT were prepared in ethanol and stored at 4 °C. All chemicals were used as received without further purification.

2.2. Instrumentation

A Specord 500 AnalytikJena instrument was used for UV−Vis surface resonance study of the synthesized curcumin functionalized Ag NPs (CAgP). For recording UV spectrum, ethanol was chosen as the solvent and the addition of TNT was done such that the overall concentration of TNT in the cuvette, range between 10^{-13} M to 10^{-3} M. The size and morphology of the multifunctional NPs were examined JEM-2100 F high-resolution transmission electron microscope (HRTEM) (JEOL, Japan). X-ray diffraction (XRD) patterns were recorded on a Rigaku XRD-A112 X-ray diffractometer which employed Cu Kαradiation of wavelengthλ¼1.5418 Å to determine the phase crystallinity and purity of functionalized Ag NPs. The operating current and voltage were kept at 40 mA and 40 kV, respectively. A 2θ range from 10° to 90° was covered in steps of 0.021 with a count time of 2 s. DLS measurements were performed using Nanotrac instrument. Renishaw Raman RM 1000 spectrometer (Renishaw plc, Gloucestershire, UK), equipped with a Leica research microscope was employed for recording normal Raman (NR) and SERS spectra. A 20X magnifying lens having the capability of forming about 2 mm diameter laser spot was used for analysis. Two-laser excitation lines, near infrared (NIR) diode laser (785 nm) and argon ion laser (514.5 nm) were used for SERS analysis of

explosives molecules. Origin 8.0 has been used for data and spectral mining of the Raman spectrometer data. The synthesized sample (CAgP) has been taken as controlled and was reference subtracted in the TNT analysis.

2.3. Synthesis of curcumin functionalized Ag NPs (CAgP)

The synthesis of CAgP was performed in a two stage reaction. Firstly, PVP capped Ag NPs were synthesized which were used further for subsequent synthesis of curcumin functionalized PVP capped Ag NPs.

2.3.1. Synthesis of PVP capped Ag NPs

PVP capped Ag NPs were synthesized using modified Yugang method [25]. Briefly, 60 mg AgNO$_3$ and 300 mg PVP were added into a three-necked flask containing 20 mL EG under vigorous stirring. EG act here as a reducing agent, capping agent as well as solvent system in the reaction. The mixture was heated in an oil bath and the solids gradually dissolved. After complete dissolution, the mixture was maintained at 140 °C for 10 min and the solution turned red. The separation and purification of the as synthesized Ag NPs was done by adding the excess of acetone to it and standing the whole solution overnight. The as synthesized PVP capped Ag NPs found to be settled at the bottom, which is separated by centrifugation at a speed at a moderate speed of 5000 r.p.m. It was further purified by washing with acetone subsequently in a repeated manner. The obtained purified NPs were air dried and used for further process. i.e. for functionalization of it by curcumin molecules.
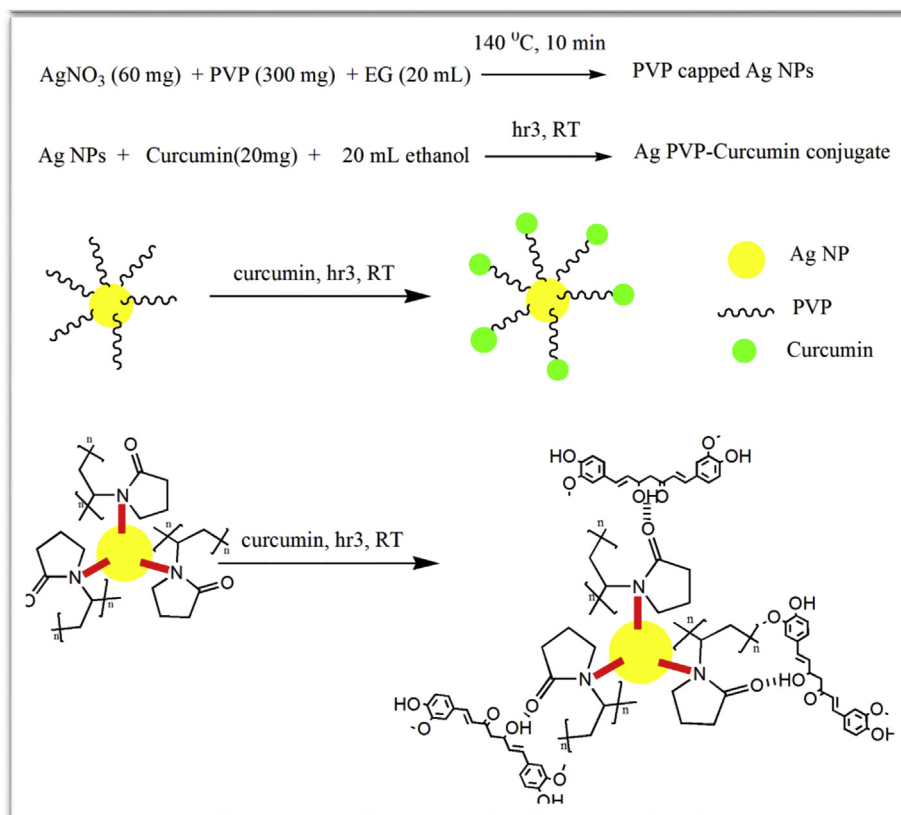
2.3.2. Synthesis of curcumin functionalized PVP capped Ag NPs (CAgP)

For conjugation of curcumin to PVP capped Ag-NPs, 20 mg of crystalline curcumin was dissolved in 25 ml ethanol and this solution was added to the 100 ml of PVP capped silver nanoparticles in ethanol under stirring at room temperature. Further this mixture was stirred for 3 h at 30 °C and then cooled down to room temperature. The use of ethanol allowed us to have more curcumin in the solution since curcumin solubility is meager in aqueous solution and also help in separation & purification during the later stages due to its low boiling point. The Ag−curcumin solution was then centrifuged at 6000 r.p.m to remove unattached curcumin. The centrifugation was done at least for three times to ensure that no free curcumin molecules are left in the final conjugate. The final solution was used for spectroscopic study and TEM analysis. Part of this solution was evaporated under vacuum using a rotary evaporator and then the remnant was centrifuged to obtain the powder, which was further used for SERS analysis. The as synthesized PVP capped Ag-NPs were stored in a brown glass vial in a refrigerator as there is abundance of precedence literature which has established that exposure to light will oxidized the Ag Np's and exposure to higher temperature will oxidized curcumin.

The schematic representation for the synthesis of PVP capped curcumin functionalized Ag NPs is shown in Fig. 1.

2.4. SERS measurements

For SERS analysis using CAgP, an argon ion laser (514.5 nm) was used. 4 μL of the analyte to be detected i.e. TNT, 2,4 DNT, phenol, p-nitrobenzaldehyde, nitrobenzene etc. was put on glass slide followed by addition of 4 μL of curcumin Ag NPs alcoholic solution. The solution was allowed to dry before recording the SERS spectra. The SERS spectrum was recorded in triplicate.

Fig. 1. Schematic representation for the synthesis of PVP capped curcumin functionalized Ag NPs.

2.5. Results and discussion

2.5.1. Characterization of curcumin functionalized PVP capped Ag NPs (CAgP)

The as synthesized CAgP were characterized by U.V–Vis, IR, XRD, DLS and TEM techniques. The reddish color of the Ag NPs colloid and the UV–Vis peak maxima at 409 nm indicate the formation of silver nanoparticles. Fig. 2a showed the UV spectra of Ag-NPs with a surface plasmon peak centered at 409 nm. The SPR peak formation and its sharpness have been widely used in literature for nanoparticles formation confirmation and the particle size distribution. The sharp UV peak signifies the uniform particle size distribution. TEM image showed that the NPs are highly dispersed and majority of them are spherical in shape (Fig. 2b). The crystallinity and phase purities of the as-prepared functionalized Ag NPs were examined by powder X-ray diffraction (XRD). Fig. 2c showed the XRD pattern of the NPs. The pattern of the sample matched well with the standard XRD reflection patterns of silver (JCPDS file No. 04–0783). All of the peaks of the patterns of the sample can be readily indexed to face centered-cubic silver (JCPDS file No. 04–0783), where the diffraction peaks at 2θ values of 38.24, 44.42, 64.44, 77.40° can be ascribed to the reflection of (111), (200), (220), (311) planes of the face-centered cubic silver, respectively. No peaks from other phases were detected, indicating high purity of the Ag NPs. The DLS measurement further confirmed the uniform particle distribution as the majority of particles are found to be 52 ± 2 nm in size. Fig. 2d showed the DLS spectra of curcumin functionalized Ag NPs.

Fig. 3 showed the FTIR spectra of (a) curcumin (b) PVP and (c) curcumin functionalized PVP capped Ag NPs. Here spectra (a) and (b) show the typical signatures of both curcumin and PVP. Signature peaks of curcumin are free O–H group (3435 cm^{-1}), C–O and

C–C(enol)(1450–1630 cm^{-1}), C–H(methyl)(2845 cm^{-1}), C–H (aryl) (3015 cm^{-1})and C–O–C(1000–1300 cm^{-1}) typically attributed to symmetric and asymmetric configurations of C–O–C chains [31,32]. The signature peaks in PVP spectra may be recognized as C–O (1660 cm^{-1}) and C–N (1290 cm^{-1}), (iv) shows the conjugation of curcumin with PVP capped Ag NPs [32]. This figure reveals signatures of both PVP and curcumin molecule conjugated to Ag NPs. PVP may attach to Ag NPs via oxygen or nitrogen atom, thus enabling the other free one to form intermolecular H-bonding with enolic hydroxyl group. Fig. 4 showed the possible binding sites for PVP to Ag NPs. Curcumin molecule may attach to the PVP capped Ag NPs with intermolecular hydrogen bonding to enolic hydroxyl group which results in shift of O–H stretching from 3435 cm to 1–3402 cm^{-1} whereas the basic diaryl heptanoid group, which is the chromophore group of curcumin remains intact [32].

The curcumin conjugation is also evident in the form of shift of C–O stretching of PVP from 1660 cm^{-1}–1646 cm^{-1}. The curcumin conjugate with PVP is depicted in Appendix A1. It is clear from the A1 that conjugate is possible due to H-bonding of enolic hydroxyl group with oxygen atom of PVP.

When PVP is attached via oxygen atom, H-bonding occurred between enolic hydroxyl groups of curcumin with nitrogen atom of the PVP. The very similar observations has been made by Datar et al. [31], who have described conjugation of curcumin with PVP capped citric acid reduced gold nanoparticles for improving curcumin's bioavailability. They have also suggested PVP binding to Au NPs via both oxygen and nitrogen atom.

2.5.2. SERS detection of TNT explosive using curcumin functionalized PVP capped Ag NPs (CAgP)

Our method for detection of TNT relied upon the aggregation of NPs by incorporating a specific chemical moiety on the SERS active
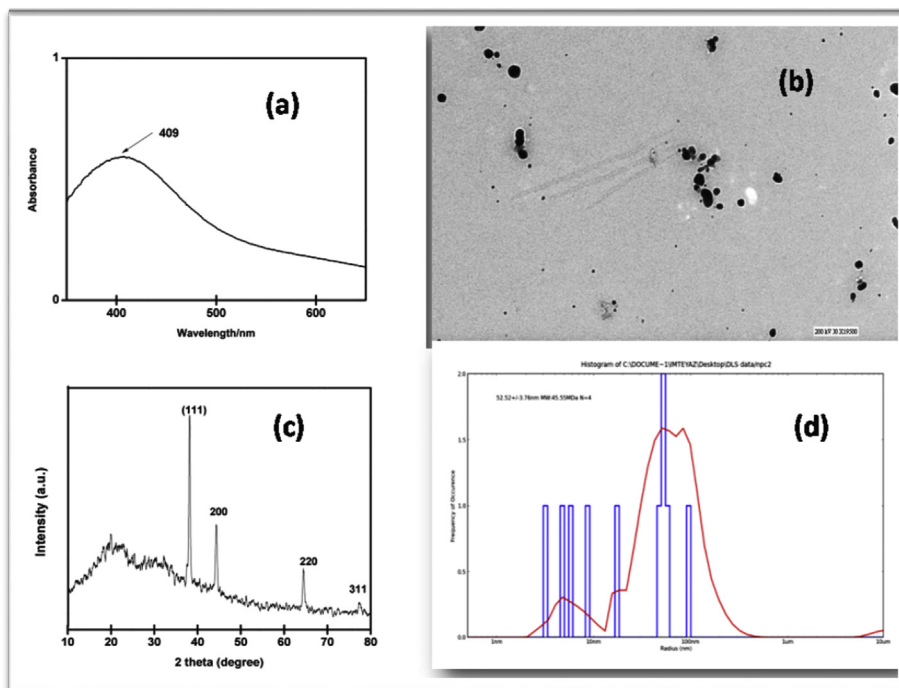
Fig. 2. NPs characterization (a) U.V. spectrum, (b) TEM image, (c) XRD spectrum and (d) DLS spectrum.
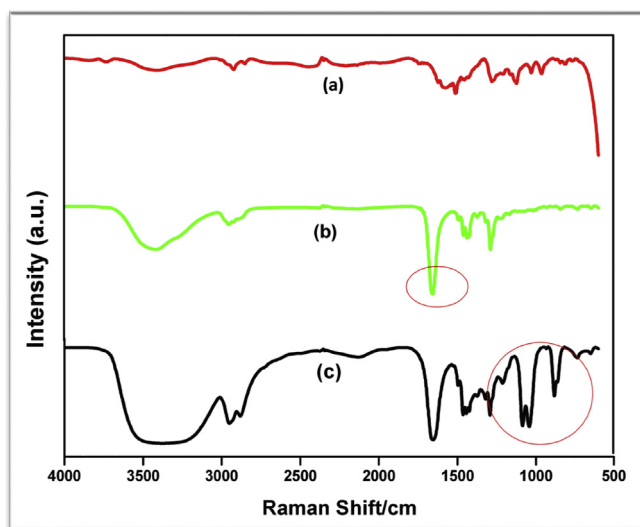

Fig. 3. IR spectra of (a) curcumin, (b) PVP and (c) curcumin functionalized Ag NPs.

NPs surface, such that there is strong interaction between the TNT molecules and the chemical moiety present on SERS active NPs surface. The selection of Ag NPs for the surface functionalization was done as there are many reports in the past which confirmed the superior SERS activity of Ag NPs as compared to other SERS active NPs. In our investigation, we evaluated the interaction between TNT and curcumin functionalized Ag NPs by electronic absorption, DLS and SERS study. During study, we found that trace amounts of TNT interact with curcumin functionalized Ag NPs and the NPs undergo aggregation because of the p-donor-acceptor interactions between TNT and curcumin present on NPs surface.

2.5.2.1. UV—vis study of the interaction of CAgP with TNT molecule.
To study the interaction between CAgP and the TNT molecule

which caused aggregation, firstly UV—Vis analysis has been done as it is well documented that the SPR peak position & intensity depends directly on the nanoparticles size distribution. The increased aggregation of NPs will resulted in shift of SPR peak or decrease in its intensity. It has been done by the addition of different concentration of TNT to the colloidal solution of the curcumin functionalized Ag NPs and recording the U.V spectra after each addition. Appendix A2 showed the U.V spectrum of CAgP after successive addition of TNT to the CAgP colloid.

It is evident from the UV spectra (A2) that pure CAgP showed sharp SPR peak centered at around 509 nm. When TNT was added to the same colloid the SPR peak appeared to diminish with increasing TNT concentration and almost disappeared at the TNT concentration of 10^{-3} M. At higher concentration, the naked eye visible flakes floating in the cuvette were observed. The disappearance of SPR peak can be explained in the terms of aggregation of curcumin Ag NPs. As the concentration of TNT is increased the size of aggregates increased. The SPR peak depends upon the size of aggregate and it is reported to diminish when particles reached in micrometers range. When we added TNT to CAgP, it undergoes aggregation due to the strong p-donor—acceptor interaction between electron deficient TNT and electron rich curcumin present on Ag NPs surface. These interactions bring CAgP close to each and resulted in aggregation.

The formation of an energy transfer (ET) complex between p-electron rich curcumin present on Ag NPs and electron deficient nitroaromatic TNT which resulted in aggregation of it was further supported by transmission electron microscopy (TEM) study. Fig. 5 showed the TEM and optical images of the CAgP with different concentration of TNT added to them.

It is observed from the image that the pure CAgP are highly dispersed and found to be of average size 50 ± 2 nm. With the addition of TNT at 10^{-9} M & 10^{-7} M the rate of aggregation increases, as evident by the large population of NPs in the same area as of pure curcumin Ag NPs. These particles continue to aggregate with more concentration of TNT addition. When the overall
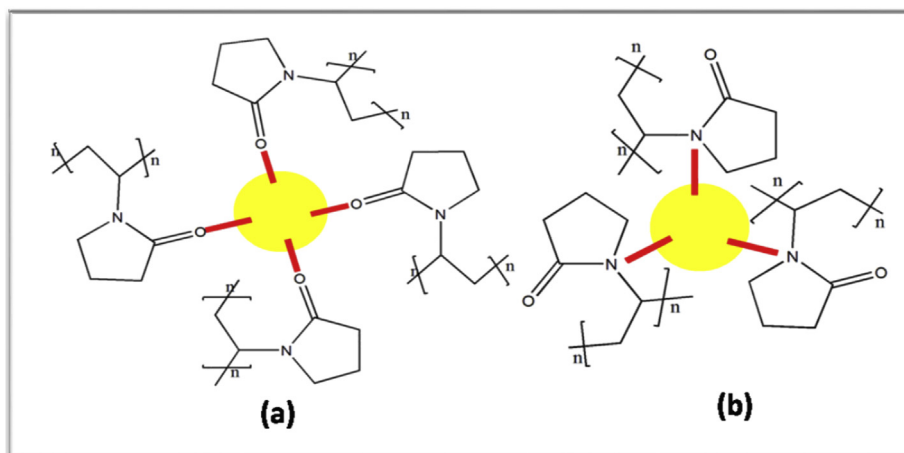
Fig. 4. Possible bonding of PVP molecule to Ag NPs via (a) oxygen atom and (b) nitrogen atom. The yellow sphere defined Ag NPs while the red bond illustrates the attachment between Ag NPs and PVP molecule. (For interpretation of the references to color in this figure legend, the reader is referred to the Web version of this article.)
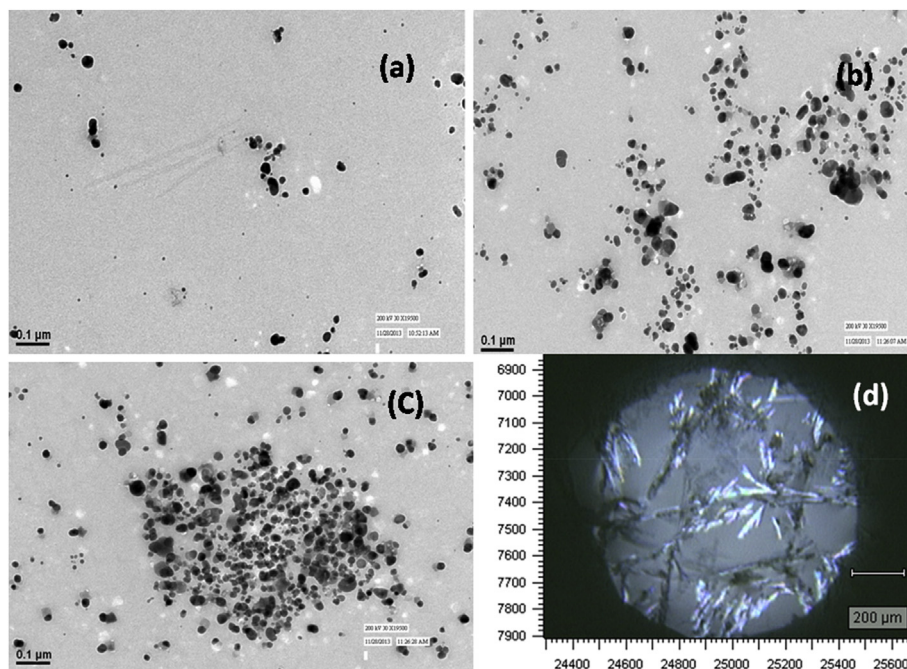

Fig. 5. TEM images of (a) pure curcumin Ag NPs colloid (b) after addition of TNT [10^{-9} M], (c) addition of TNT [10^{-6} M] and optical microscope image after addition of TNT [10^{-3} M].

concentration of TNT reached 10^{-3} M, the aggregated NPs in form of flakes can be seen even with naked eyes. Fig. 6d is an image captured with Leica Raman research microscope at the magnification of 10X. The aggregation of curcumin Ag NPs with the addition of TNT is a time dependent process. Appendix 3 showed the UV spectra of curcumin Ag NPs after addition of TNT [10^{-3} M] at different time (in seconds). The aggregation process proved to be a rapid process with initiation of aggregation started within 5 s after the addition of TNT. The process of aggregation is completed within 180 s and hence making it one of the rapid processes for the naked eye detection of TNT at trace level.

2.5.2.2. DLS study of the interaction of CAgP with TNT molecule.
The aggregation of CAgP upon the addition of TNT molecules is also supported by the DLS measurement. Appendix A4-A7 showed the DLS measurements for pure CAgP and after addition of TNT in

varying concentrations to it. The average particle size of the pure CAgP as measured by DLS comes out to be 52 ± 2 nm, which is in accordance with the TEM study. On contrast, when TNT was added to the CAgP solution in varying concentration i.e. 10^{-11} M, 10^{-9} M and 10^{-5} M, the DLS measurement showed the agglomeration of the Ag NPs which is evidenced by the increase in average particle size. It showed average particle size of 52 nm, 120 nm, 1 μm & 5 μm for the TNT concentration ranging from zero, 10^{-11} M, 10^{-9} M and 10^{-5} M respectively. As observed in UV study, naked eye visible flakes of CAgP were formed at the concentration of TNT higher than 10^{-4} M in DLS study also.

2.5.2.3. SERS study of the interaction of CAgP with TNT molecules.
The aggregation of CAgP upon addition of TNT molecules prompted us to made SERS study of the system, as it is well documented in the literature that during the aggregation, Ag NPs come close to each
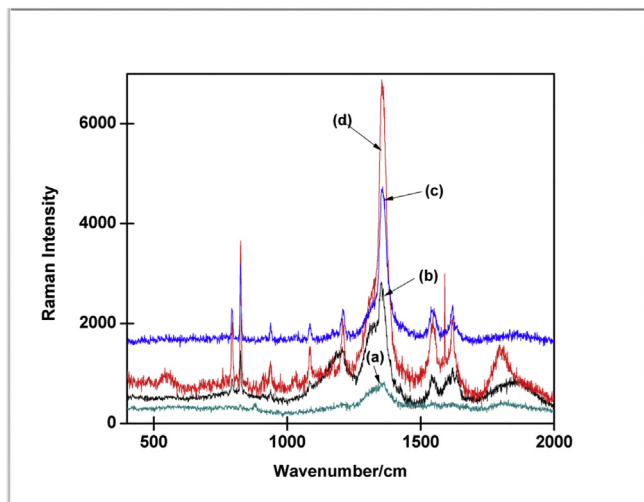
Fig. 6. SERS measurements for TNT detection using curcumin Ag NPs colloid (a) TNT [10^{-11} M], (b) TNT [10^{-7} M] (c) TNT [10^{-5} M] and (d) TNT [10^{-3} M].

Fig. 7. Change in the U.V–Vis spectra of curcumin Ag NPs after addition of different analytes in equimolar concentration to it. TNT is trinitrotoluene, DNT is dinitrotoluene, NB is nitrobenzaldehyde, PH is phenol, CAgP is curcumin Ag NPs and p-BA is para-benzaldehyde.

other creating 'hot-spots' for the SERS analysis [33]. The aggregation creating 'hot-spots' has been held mainly responsible for the highly enhanced SERS spectra of the concerned molecule bind to the Ag NPs surface. Fig. 6 showed the SERS spectra of TNT at different concentrations.

It is evident from the NR and SERS spectrum of TNT that the SERS spectrum of TNT is not only enhanced in term of increase in peak intensity, but also some new peaks which were negligible in the NR (Normal Raman) spectrum were observed in SERS spectrum. NR spectra of solid TNT is provided in Appendix A8. The tentative peaks assignment for TNT is provided in Appendix A9. It was found that peaks in NR and SERS spectra were identical with a little shifting of peaks. The peaks observed were found to be accorded to the literature [34].

The Raman spectrum of CAgP is provided in Appendix A10. The A10 contained the signature Raman peaks of curcumin and PVP in accordance with the literature.

2.5.2.4. Selectivity study of CAgP for detection of TNT molecules. To test the selectivity of the CAgP for the detection of TNT, U.V–Vis experiments have been done with other nitrated molecules and some other molecules which could act as interferrent. Fig. 7 showed the change in the U.V–Vis spectra of CAgP after addition of some common interferrents to it. The selectivity could be measured as a change in the absorbance SPR peak of the CAgP after addition of these molecules.

Our experimental results clearly show that CAgP do not undergo aggregation in the presence of other nitro compounds and common interferrents like p-nitrobenzoic acid, phenol, nitrophenol and p-benzaldehyde. This may be due to lack of electron deficiency in these molecules which is the pre-requisite condition to form strong p-donor–acceptor interactions like TNT with curcumin AgNPs, and as a result, the aggregation of curcumin Ag NPs is prevented. Although a significant decrease in the absorbance of CAgP was observed when dinitrotoluene (DNT) was used, it is not at par with TNT. So our probe clearly shows the excellent selectivity for the detection of TNT over the other nitrated molecules and common interferrents.

The schematic representation for the TNT induced aggregation
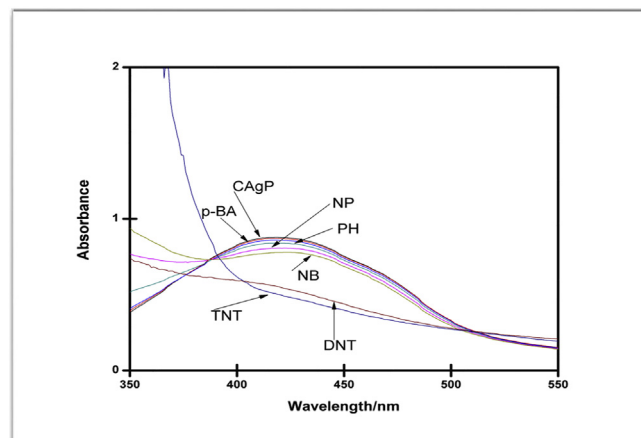
of CAgP which helped us in the detection of TNT at ultra trace level by U.V–Vis, DLS and SERS method is shown in Fig. 8.

It is clear from Fig. 8 that as the concentration of TNT is increased the CAgP come close to each other forming aggregates which form the basis for the detection of TNT using U.V–Vis., DLS & SERS method. The introduction of PVP on Ag NPs followed by curcumin attachment to it increase the stability of the overall CAgP, as the curcumin degrade very rapidly on the bare Ag NPs [35].

2.5.2.5. Stability study of CAgP for detection of TNT molecules. The synthesized CAgP were stored in a brown glass vial under refrigerated conditions to minimize the degradation of curcumin and self aggregation of Ag Np's. To study the shelf life the synthesized CAgP, SERS spectra of 10^{-3} M TNT was recorded after one and three months. It was found out that there was negligible loss in the SERS activity of CAgP during the storage of one month. An appreciable loss in the intensity of peaks as well as the quantity of signature peaks of TNT was observed during the storage of CAgP for three months (Appendix A11). The significant loss could be attributed to the degradation of curcumin due to oxidation [36]. It is recommended to utilize the CAgP within the one month of its synthesis.

3. Conclusions

In conclusion, in this paper, we have demonstrated for the first time a curcumin functionalized Ag NPs based, highly selective, and ultrasensitive U.V, DLS & SERS based multiple tier, real time probe for the detection of TNT up to 0.1 nM level. The utmost significance of the synthesized curcumin Ag NPs lie in its ability to detect TNT at multiple levels using U.V–Vis., DLS and SERS methods. The as synthesized CAgP made possible the naked eye detection of TNT in the form of visible CAgP flakes. The recent advancements in portable Raman spectrometers and its widespread use at airports etc. for security reasons combined with the simplicity, speed, and sensitivity of this approach, the developed method could easily be extended to a high-throughput format and become a common method of choice for the fast and reliable detection of explosives for screenings in airports, analysis of forensic samples, and environmental analysis.
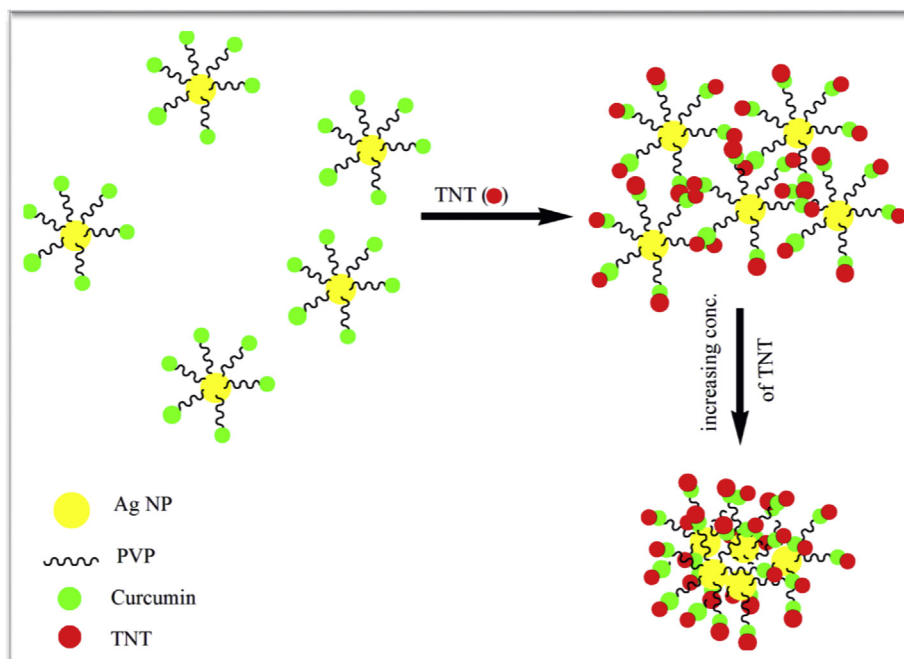
Fig. 8. Schematic illustration for aggregation of curcumin Ag NPs by addition of TNT.

CRediT authorship contribution statement

Ali Raza: conceptualization, data curation, analysis, experimentation, manuscript preparation, software, visualization, validation, original draft, review & editing. **Amitabh Biswas:** methodology, investigation, software, review & editing. **Abdurrohman Mengesha:** methodology, supervision, validation, review & editing.

Declaration of competing interest

The authors declare that they have no known competing financial interests or personal relationships that could have appeared to influence the work reported in this paper.

Appendix A. Supplementary data

Supplementary data to this article can be found online at https://doi.org/10.1016/j.fsisyn.2020.08.001.

References

[1] J. Yinon, Forensic and Environmental Detection of Explosives, John Wiley & Sons, 1999.
[2] Y. Wang, A. La, Y. Ding, Y. Liu, Y. Lei, Novel signal-amplifying fluorescent nanofibers for naked-eye-based ultrasensitive detection of buried explosives and explosive vapors, Adv. Funct. Mater. 22 (2012) 3547—3555.
[3] J. Yinon, Field detection and monitoring of explosives, Trac. Trends Anal. Chem. 21 (2002) 292—301.
[4] D.F. Rendle, Advances in chemistry applied to forensic science, Chem. Soc. Rev. 34 (2005) 1021—1030.
[5] J.S. Caygill, F. Davis, S.P.J. Higson, Current trends in explosive detection techniques, Talanta 88 (2012) 14—29.
[6] M. López-López, C. García-Ruiz, Infrared and Raman spectroscopy techniques applied to identification of explosives, Trac. Trends Anal. Chem. 54 (2014) 36—44.
[7] M.E. Germain, M.J. Knapp, Optical explosives detection: from color changes to fluorescence turn-on, Chem. Soc. Rev. 38 (2009) 2543—2555.
[8] S. Singh, Sensors—an effective approach for the detection of explosives, J. Hazard Mater. 144 (2007) 15—28.
[9] V.K.K. Upadhyayula, Functionalized gold nanoparticle supported sensory mechanisms applied in detection of chemical and biological threat agents: a review, Anal. Chim. Acta 715 (2012) 1—18.
[10] A.M. Jimenez, M.J. Navas, Chemiluminescence detection systems for the analysis of explosives, J. Hazard Mater. 106 (2004) 1—8.
[11] A. Lan, K. Li, H. Wu, D.H. Olson, T.J. Emge, W. Ki, M. Hong, J. Li, A luminescent microporous metal—organic framework for the fast and reversible detection of high explosives, Angew. Chem. Int. Ed. 48 (2009) 2334—2338.
[12] A. Hakonen, P.O. Andersson, M.S. Schmidt, T. Rindzevicius, M. Käll, Explosive and chemical threat detection by surface-enhanced Raman scattering: a review, Anal. Chim. Acta 893 (2015) 1—13.
[13] W. Sara, A. Pettersson, H. Östmark, A. Hobro, Laser-based standoff detection of explosives: a critical review, Anal. Bioanal. Chem. 395 (2009) 259—274.
[14] S.S.R. Dasary, D. Senapati, A.K. Singh, Y. Anjaneyulu, H. Yu, P.C. Ray, Highly sensitive and selective dynamic light-scattering assay for TNT detection using p-ATP attached gold nanoparticles, ACS Appl. Mater. Interfaces 12 (2010) 3455—3460.
[15] A. Pandya, H. Goswami, A. Lodha, S.K. Menon, A novel nanoaggregation detection technique of TNT using selective and ultrasensitive nanocurcumin as a probe, Analyst 137 (2012) 1771—1774.
[16] B.D. Piorek, S.J. Lee, M. Moskovits, C.D. Meinhart, Free-surface microfluidics/surface-enhanced Raman spectroscopy for real-time trace vapor detection of explosives, Anal. Chem. 84 (2012) 9700—9705.
[17] A.R. Alvarez-Puebla, L.M. Liz-Marzan, Traps and cages for universal SERS detection, Chem. Soc. Rev. 41 (2012) 43—51.
[18] J.M. Sylvia, J.A. Janni, J.D. Klein, K.M. Spencer, Surface-enhanced Raman detection of 2, 4-dinitrotoluene impurity vapor as a marker to locate landmines, Anal. Chem. 72 (2000) 5834—5840.
[19] A. Raza, B. Saha, In situ silver nanoparticles synthesis in agarose film supported on filter paper and its application as highly efficient SERS test stripes, Forensic Sci. Int. 237 (2014) e42—e46.
[20] C.H. Lee, L. Tian, S. Singamaneni, Paper-based SERS swab for rapid trace detection on real-world surfaces, ACS Appl. Mater. Interfaces 12 (2010) 3429—3435.
[21] A. Tao, F. Kim, C. Hess, J. Goldberger, R. He, Y. Sun, Y. Xia, P. Yang, Langmuir—Blodgett silver nanowire monolayers for molecular sensing using surface-enhanced Raman spectroscopy, Nano Lett. 9 (2003) 1229—1233.
[22] S.S. Dasary, A.K. Singh, D. Senapati, H. Yu, P.C. Ray, Gold nanoparticle based label-free SERS probe for ultrasensitive and selective detection of trinitrotoluene, J. Am. Chem. Soc. 131 (2009) 13806—13812, 2009.
[23] S. Botti, L. Cantarini, A. Palucci, Surface-enhanced Raman spectroscopy for trace-level detection of explosives, J. Raman Spectrosc. 41 (2010) 866—869.
[24] S. Devi, B. Singh, A.K. Paul, S. Tyagi, Highly sensitive and selective detection of trinitrotoluene using cysteine-capped gold nanoparticles, Anal. Methods 8 (2016) 4398—4405.
[25] Y. Sun, Y. Xia, Shape-controlled synthesis of gold and silver nanoparticles, Science 298 (2002) 2176—2179.
[26] T. Liyanage, A. Rael, S. Shaffer, S. Zaidi, J.V. Goodpaster, R. Sardar, Fabrication of a self-assembled and flexible SERS nanosensor for explosive detection at parts-per-quadrillion levels from fingerprints, Analyst 143 (2018) 2012—2022.

[27] R. Gillibert, J.Q. Huang, Y. Zhang, W.L. Fu, M.L. de la Chapelle, Explosive detection by surface enhanced Raman scattering, Materials 105 (2018) 166—172.

[28] S. Emamian, A. Eshkeiti, B.B. Narakathu, S.G.R. Avuthu, M.Z. Atashbar, Gravure printed flexible surface enhanced Raman spectroscopy (SERS) substrate for detection of 2,4-dinitrotoluene (DNT) vapor, Sensor. Actuator. B Chem. 217 (2015) 129—135.

[29] A.K.M. Jamil, E.L. Izake, A. Sivanesan, P.M. Fredericks, Rapid detection of TNT in aqueous media by selective label free surface enhanced Raman spectroscopy, Talanta 134 (2015) 732—738.

[30] S. Ben-Jaber, W.J. Peveler, R. Quesada-Cabrera, C.W.O. Sol, I. Papakonstantinou, I.P. Parkin, Sensitive and specific detection of explosives in solution and vapour by surface-enhanced Raman spectroscopy on silver nanocubes, Nanoscale 9 (2017) 16459—16466.

[31] R.K. Gangwar, V.A. Dhumale, D. Kumari, U.T. Nakate, S.W. Gosavi, R.B. Sharma, S.N. Kale, S. Datar, Conjugation of curcumin with PVP capped gold nano-particles for improving bioavailability, Mater. Sci. Eng. 32 (2012) 2659—2663.

[32] S.M. Phumlani, N.M. Sosibo, P.N. Mashazi, T. Nyokong, R.T. Tshikhudo, A. Skepu, Elma van der Lingen, Selective adsorption of PVP on the surface of silver nanoparticles: a molecular dynamics study, J. Mol. Struct. 1004 (2011) 131—137.

[33] L. Sun, Y. Song, L. Wang, C. Guo, Y. Sun, Z. Liu, Z. Li, Ethanol-induced formation of silver nanoparticle aggregates for highly active SERS substrates and application in DNA detection, J. Phys. Chem. C 112 (2008) 1415—1422.

[34] J. Clarkson, W.E. Smith, D.N. Batchelder, D.A. Smith, A.M. Coats, A theoretical study of the structure and vibrations of 2, 4, 6-trinitrotolune, J. Mol. Struct. 648 (2003) 203—214.

[35] M.V. Canamares, J.V. Garcia-Ramos, S. Sanchez-Cortes, Degradation of curcu-min dye in aqueous solution and on Ag nanoparticles studied by ultraviolet—visible absorption and surface-enhanced Raman spectroscopy, Appl. Spectrosc. 60 (2006) 1386—1391.

[36] K.I. Priyadarshini, The chemistry of curcumin: from extraction to therapeutic agent, Molecules 19 (2014) 20091—20112.